Journal of Radioanalytical Chemistry, Vol. 12 (1972) 39—52

Microtechniques

PROTON MICROBEAMS, THEIR PRODUCTION AND USE

J. A. COOKSON, A. T. G. FERGUSON, F. D. PILLING

Nuclear Physics Division, AERE, Harwell, Nr. Didcot, Berks. (England)

Well focused beams of protons and other ions provide a very powerful means of determining how the elemental composition of a sample varies over its surface. Observation of the X-rays from proton bombardment can provide great sensitivity in most cases, while detection of nuclear effects has special applicability for elements of low atomic weight. A focusing system using high precision magnetic quadrupoles was designed and built for use with the IBIS 3 MeV Van de Graaff generator. Measurements of the first order focusing and aberrations agreed satisfactorily with theoretical predictions. The focused beam of 3 MeV protons was measured to have a diameter of less than 4 μm. The target chamber, deflection system and display system are described and examples given of use of the system. Backgrounds in X-ray detection are discussed and limits of detection are given.

Introduction

The principle has been well established of carrying out analysis by the study of the secondary radiations emitted when thin films or surfaces are bombarded with charged particles whether they be electrons, protons or heavier ions. Clearly, if the area irradiated can be made small, the spatial distribution of elements can be determined with high resolution. Before the work which will be described below, such fine resolutions had not been obtained for protons. Electrons can readily be focussed to beam diameters of less than 1 μm though multiple scattering in the sample raises the effective diameter to 2 μm. This is done using axially symmetric electrostatic or magnetic lenses which have been intensively studied and developed for the field of electron microscopy. The maximum yield of K X-rays is excited by electrons of energy 3 times the K shell ionization energy. This means that a beam of energy of <100 KeV can strongly excite characteristic radiation. Cross sections at peak are for example $40 \cdot 10^{-24}$ cm^2 for Ag and $400 \cdot 10^{-24}$ cm^2 for Ni. The disadvantage of the electron microprobe lies in the fact that an intense continuum of bremsstrahlung is produced which forms a serious background. The use of a high resolution dispersive X-ray spectrometer gives the optimum obtainable peak/background ratio. In Table 1 taken from a paper by POOLE and COOKSON we show some typical figures.

Table 1

The optimum obtainable peak/background ratio for a high-resolution dispersive X-ray spectrometer

Specimen	Electron energy, keV	Peak counts per second for 0.1 μA	Peak/background ratio
Carbon	15	3 000	300 : 1
Aluminium	25	27 000	3 000 : 1
Titanium	25	23 000	970 : 1
Iron	25	39 000	650 : 1
Copper	25	26 000	450 : 1

Clearly even under the most favourable conditions a peak/background ratio of 3 000 : 1 is the best attainable. While this performance is adequate for a great many applications, increased sensitivity is always required and this prompted the attempt to avoid the principal source of background by use of a proton beam rather than one of electrons.

The use of proton beams in determining the elemental composition of surfaces was demonstrated[1] as long ago as 1950. Since then, analysis with protons and other ion beams has included the study of elastic scattering and the production of γ-rays, neutrons, or secondary ions.[2–4] Several authors[5,6] have extended this work by using a collimated beam to study the spatial distribution of elements in surfaces. It is light elements that gave the most intense and easily recognised radiations with proton or deuteron beams of a few MeV energy, so that for example PIERCE et al.[5] have found it possible to determine concentrations of such elements as low as a few parts in 10^5. This technique compliments the proton excitation of X-rays which for light elements meets difficulties because of the absorption of the soft X-radiation.

For proton beams of a few MeV energy, yields of characteristic K X-rays per proton are comparable to those for electrons of ~25 keV. The technology of the production of proton beams of these energies by Van de Graaff type machines is well developed and their cost is comparable to that of the sophisticated spectroscopic equipment and electronics that would be common to either system. If direct proton bremsstrahlung were the sole source of background, peak-to-background ratios would be expected to be in excess of 10^6 : 1. POOLE and SHAW[7] have made measurements using a 2.5 MeV proton beam on an aluminium target in which, even under adverse circumstances, a peak-to-background ratio of $4 \cdot 10^4$: 1 was observed and they argue plausibly that with realistic improvements in their equipment a ratio of $2.5 \cdot 10^5$: 1 for aluminium should be obtainable.[7,8] These figures were sufficiently encouraging to proceed with the development of a proton microbeam.

The production of a proton microbeam

To handle a beam of 3 MeV protons with magnetic lenses of the cylindrical type conventionally used in electron microscopes and microprobes would be quite impracticable. For low energy heavy ions, e.g. 30 keV argon ions, electrostatic lenses have been used very successfully,[9] but practical limitations appear rapidly with increase in the beam energy. The natural resort is to consider strong focusing with quadrupole lenses, although hitherto the main use of these devices in work of high positional resolution has been as correctors of aberration in conventional lens systems.[10]

The present work uses a quadrupole lens system of the type known as the Russian quadruplet, whose first order properties were studied by DYMNIKOV et al.[11] In this system the four quadrupoles are alternately focusing and defocusing in a particular plane and the first and fourth lenses have equal strength ($\beta_1 L_1$ in DYMNIKOV's notation) as have the second and third ($\beta_2 L_2$). Because of its symmetry such a system is orthomorphic, i.e. with the image the same shape as the object. A plot of $\beta_1 L_1$ against $\beta_2 L_2$ for focusing was shown by DYMNIKOV to have several branches corresponding to different types of path through the system, some with quite wild oscillations of the beam profile. Branch 1, for which the beam deviates only comparatively gently, was considered by HAWKES and MEADS.[12] They calculated all the aberration coefficients for a system with the quadrupoles in contact and the second and third ones of about twice the length of the other two. For a parallel incident beam focused to a point at the end face of the last quadrupole they obtained a value of C_s/f of 32, where C_s is defined as the largest of the third order aperture aberration coefficients and f is the focal length. The implications of such an aberration constant applied to the slightly different geometry of the present experimental system will be considered later.

Each of the four quadrupoles used in almost all of this work had an aperture diameter (pole tip to pole tip) of 3.84 cm, a geometrical length of 18.05 cm and soft iron poles which were sections of cylinders with diameters of 4.42 cm. There were 3 250 turns of copper wire per pole and cooling water passed through jackets attached to the coils. Each quadrupole was excited by a power supply capable of giving up to 1 A with a stability of $\pm 0.01\,\%$.

It was clear[10,13] that in order to achieve good focusing it would be necessary to minimize imperfections in the symmetries of the magnetic field and this implied accuracy in the geometry of the individual quadrupoles and in their relative positions. Measurements showed that averaging over the four lenses the distances between the two pairs of opposite poles differed by only ± 0.013 mm and that the average variation in the shortest distance between neighbouring poles on a single magnet was ± 0.045 mm in 14.25 mm. To facilitate relative rotations of the quadrupoles without affecting their alignment they were mounted with their yokes, which were of cylindrical form, on two rows of rollers. Neighbouring quadrupoles were mounted 4.5 cm apart. By use of a telescope and a graticule placed in turn at each end of each lens, the set of quadrupoles was put onto a com-

mon geometrical axis to an accuracy of about $\pm 50\ \mu$m. The magnetic centres of the four quadrupoles were then checked using the technique of COBB and MURRAY[14] and shown to coincide with the geometrical centres within the method's accuracy limit of about $\pm 130\ \mu$m.

Fig. 1(a) shows the layout of the experiment. The proton beam was produced by the Harwell Nuclear Physics Division's 3 MeV Van de Graaff generator IBIS.

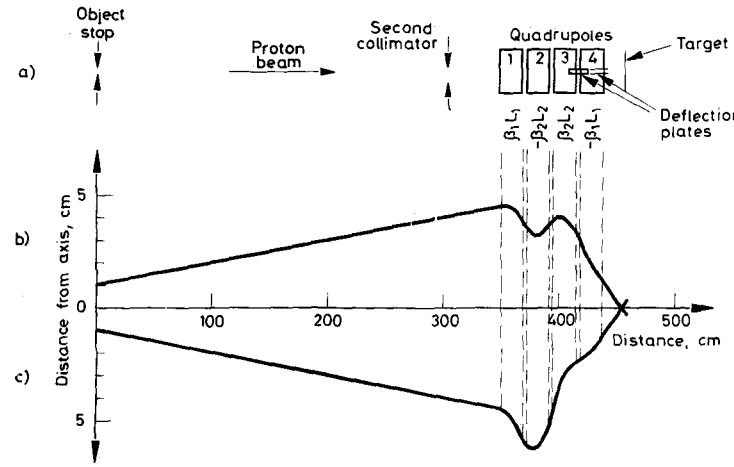

Fig. 1. a — The layout of the focusing system; b — Calculated trajectory in the horizontal plane for ray starting 1 cm from the axis with 0.01 radian divergence; c — Calculated trajectory in the vertical plane

Immediately after the machine stabilizing slits was placed the aperture which was to be the object for the focusing system. A turret system made it possible to choose any one of five holes from about 19 μm diameter upwards, drilled in tantalum discs.* The first lens of the Russian quadruplet was situated 3.5 m from the object aperture and shortly after a second set of variable apertures with a range of holes from 1.6 mm diameter upwards. The position of the target for the microbeam could be varied fairly easily but most measurements were made with the target 21.0 cm from the exit from the last quadrupole. Computer calculations using the TRAMP programme[15] assuming that the smaller aperture quadrupoles had an effective length[16] of 20.15 cm, indicated the magnetic strengths which would give the image at the appropriate position. Fig. 1(b) and (c), show, respectively, the trajectories in the vertical and horizontal planes for unit initial displacement and angular deviation. The focal length obtained for the system was 60.5 cm and the magnification 0.178. Increase of the strength of the quadrupoles could produce smaller images but a limiting magnification of 0.141 would occur with the image at the exit from the last lens element.

* This arrangement has now been replaced by a high precision adjustable slit system.

To observe its size and shape during the focusing procedure the beam was allowed to strike a piece of optical quality quartz 16.5 μm thick which could be viewed by an optical microscope whose objective was inside the vacuum system with a plane glass sheet across the microscope tube acting as the limit of the vacuum. Objectives of $\times$ 10 and $\times$ 43 were available for use with a $\times$ 10 eyepiece but the latter objective had too small a depth of focus for clear observation of the glow caused by 3 MeV protons.

A simple system was used to scan the beam spot across the target plane. This consisted of two pairs of parallel plates at the positions indicated in Fig. 1(a).

Operation of the system

The set of quadrupoles was mounted on a rigid support which could be moved vertically and horizontally with adjusting screws so that, after the relative positions of the individual elements had been fixed, alignment of the whole set about

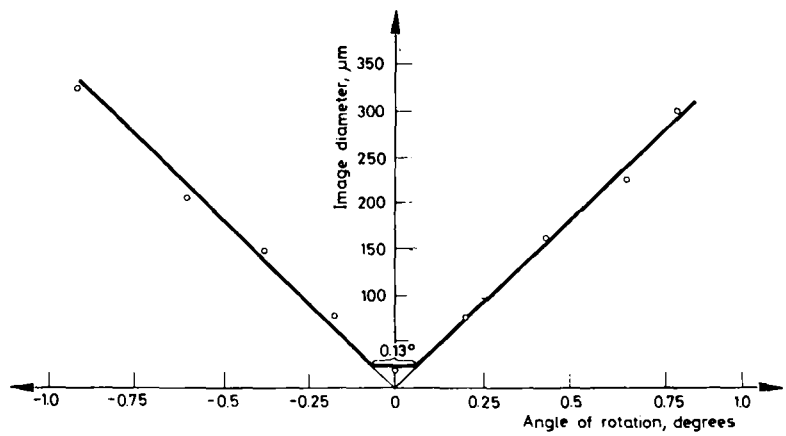

Fig. 2. Experimental measurements of the image diameter as one quadrupole is rotated away from its optimum orientation

the beam axis was fairly simple. The beam from the IBIS accelerator was arranged to aim roughly along the chosen axis and then the object aperture and machine focusing were adjusted to give optimum transmitted beam. The available current varied from day to day but 6 nA through a 28 μm aperture was fairly typical. With the quadrupoles switched off the beam image observed on a quartz 4.5 m after the aperture had an elliptical outline, which was hollow apart from a horizontal line across its centre. The size of the ellipse varied with the machine conditions but was typically 4 mm high and 8 mm wide.

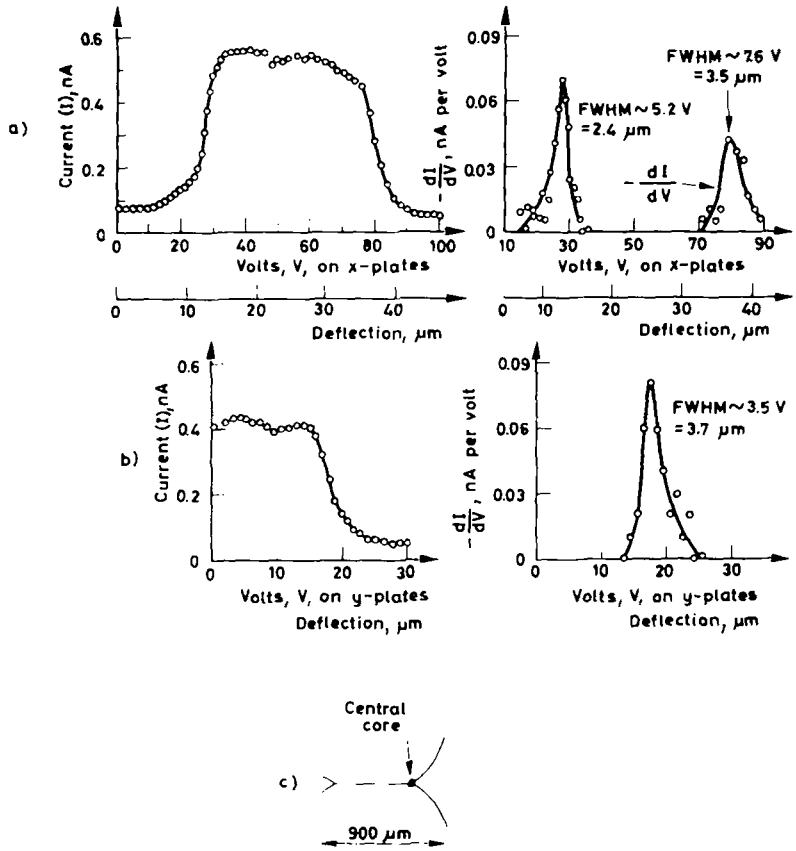

Fig. 3. The left-hand parts of (a) and (b) are the beam currents, I, observed on a copper mesh as a function of deflection voltage V, horizontally and vertically, respectively. The right-hand diagrams are the corresponding curves of dI/dV. c — An impression of the fluorescence seen on quartz for a 28 μm diameter object collimator and no other collimation

With the help of a telescope the set of quadrupoles was placed on the line joining the centre of the image on the quartz to the object stop. The final adjustment of the position of the set of quadrupoles was carried out using each element in turn and altering the nearest adjusting screws, horizontal or vertical as appropriate, until the image was seen in the microscope to pass through the line focus condition without steering. The remaining mechanical adjustment was that of the relative orientation of the quadrupoles. Attempts to produce a small image of a 50 μm object stop showed that rotation of just one quadrupole could apparently remove the aberration caused by incorrect relative orientation of all four quadrupoles. Fig. 2 shows the approximate image diameter as a function of the angle of rotation of the first quadrupole. The results appear to agree very well with a

linear relation between image size and angle, apart from a region of only about 0.13° where other effects dominate. However, a systematic approach to the rotational alignment was adopted. The orientation of one lens was taken as standard and this lens was used with the first one and then the other of the lenses of opposite polarity to produce a point focus. The orientation of each of these lenses was corrected until the image showed no twisting effect as the focus was approached. The fourth lens was then related to one of those just treated. This method was evidently somewhat imperfect as the system was still liable to require a small adjustment of any one lens in order to give its best focus.

With the system fully aligned the best focus occurred with the currents through the first and fourth lenses quite closely the same, as were those through the second and third lenses. Latterly it was found possible and convenient to link the windings of appropriate pairs or quadrupoles in series and use only two power supplies.

For an object stop of about 19 μm diameter the image had a central core too small to be measured on the microscope graticule but in addition, when there was no collimation immediately before the quadrupoles, there were very faint tails with approximately the form shown in Fig. 3(c). As collimation was tightened the beam spot lost brightness but the tails were shortened until for an aperture of only 1.6 mm no tails could be seen. The geometrical magnification of the lens system was measured using object apertures of 168 and 381 μm diameter. Clean images of these with diameters of 32.2 and 71.4 μm, respectively, were obtained so that the measured magnifications were 0.192 and 0.187 compared with the 0.178 calculated with TRAMP.

In order to measure the profile of the beam spot a copper grid of the type used in electron microscopy, consisting of copper strips about 24 μm wide outlining squares with sides of about 40 μm, was mounted in the image plane. The current read on this mesh was recorded as the beam position was varied using the deflector plates. Fig. 3(a) shows the results for a scan obtained with a fixed voltage on one of the Y-plates and the voltage on one of the X-plates varied. The intensity profile of the beam was obtained from the differences in the currents for successive voltages and is also shown in Fig. 3(a). The full widths at half maximum (FWHM) of the two peaks are equivalent to 2.4 and 3.5 μm. Similarly, in Fig. 3(b) a scan in the Y-direction is shown and this gives a FWHM value of 3.7 μm. These scans were made with no collimation of the beam at the entry to the quadrupoles but when there was a 1.6 mm aperture the FWHM in the Y-direction was 3.3 μm, while values obtained for the X-direction of scanning were 2.5 μm, 2.3 μm, 1.9 μm and 2.0 m. Although some secondary emission was in evidence its effect on measurements of spot size was probably small.

The relationship between deflection voltage and actual distance moved across a quartz was confirmed to be very linear, but appreciable deterioration of the spot was observed for large deflection. This aberration was shown to be roughly proportional to the deflection so that it could be quoted as a percentage of the deflection. For deflection with a voltage on only one plate at a time the extra aberration was about 5.5% of the lateral displacement in the X-direction and 6.7%

in the Y-direction. Using a deflection voltage made up of approximately equal but opposite potentials on the two Y-plates the aberration was only 2.7% of the displacement. More careful design of the deflector plates could greatly reduce these effects. In Fig. 3(a) the difference between the two FWHM values is just about equal to the effect contributed by the deflection system. The object stop for these measurements was initially 28 μm in diameter but after the measurements of spot size this had changed, probably due to the action of the beam, to an irregular shape of approximately 19 μm diameter. Using the measured magnification of 0.19 for the system the geometrical image should have diameter 3.6 μm.

The contribution to image size expected from third order aperture aberrations could be estimated. The greatest divergence of the beam leaving the object aperture was in the horizontal plane where its half angle, α, was 0.00089 radians. The diameter of the circle of least confusion caused by spherical aberration is expected[17] to be $1/2\ C_s\,\alpha'^2$, where α' is the angular aperture in the image plane. TRAMP gave $\alpha' = 5.62\alpha$ and a focal length, f, of 60.5 cm. Using these values and taking the HAWKES and MEADS[12] value for C_s/f of 32, the circle of least confusion was expected to have a diameter of 1.2 μm. Comparison of the measured image size with that expected from the first order theory sets an upper limit of perhaps 2 μm diameter on the contribution of aberrations. Thus the experimental value of C_s/f is certainly not much higher than and possibly even lower than that for the system calculated by HAWKES and MEADS. Also, of course, there is the same upper limit of 2 μm on aberrations due to imperfections in the geometry of the system.

In order to determine the amount of halo around the beam spot, a nickel foil backed by graphite was placed in the focal plane in such a way that nickel and graphite each occupied half the focal plane with a straight dividing line. A surface barrier detector measured the protons scattered at backward angles with a discriminator to select only those with sufficient energy to have come from the nickel. Comparison of the count rates with the beam spot deflected just onto and just off the nickel indicated that one half of the halo contained 1/60 of the counts in the core of the beam. By moving the nickel foil to the opposite side of the focal plane the other half of the halo was measured to have 1/40 of the count rate of the core. Thus, for this measurement with an object aperture of 28 μm diameter the total ratio of halo to core was about 1 : 24. This was for a second aperture of 3.2 mm diameter; without this collimation the halo would be greater. The measurements indicated that the halo stretched at least some hundreds of μm away from the core of the beam.

The proportion of beam going into halo was a source of concern and its origin was investigated. When the quadrupole system was sightly defocused the microscope showed the elliptical shape of the beam plus a surrounding bright region limited by the circular shape of the second aperture. By intercepting the inner ellipse with a rod placed across the beam, the current in this central region could be compared with that in the outer circular region. For object apertures of 28, 69 and 152 μm the outer region's current was almost a constant while that in the

ellipse changed by a factor of 60 for increasing aperture size. The results were compatible with the suggestion that the outer circle contains protons of energy sufficiently close to the beam energy to give the observed clear outline of the second aperture but not so close that they stay within the core for the condition of optimum focus. Clearly, the proportion of beam in the halo depends on the quality of the aperture edges and although quantitative figures are not yet available, the replacement of drilled apertures with slits has resulted in a substantial improvement.

The target facilities

A target chamber has been provided with facilities for fine movement of the specimen or focusing screen in three dimensions. Two microscopes are provided, one viewing from behind the specimen or focusing screen, the other viewing obliquely the face of the specimen irradiated by the beam. For analysis, three types of detector have so far been provided:

(1) A silicon surface barrier detector for detection of back-scattered protons. If greater sensitivity is required this could be an annular counter with the beam passing through its centre. So far, there has been no need for this greater sensitivity.

(2) A Si(Li) non-dispersive X-ray detector of 5 mm diameter and resolution of 250 eV. This resolution resolves adjacent elements down to $Z \sim 15$. Its efficiency is in excess of 50% between 4 keV and 30 keV and falls off slowly. However, for cesium the energy of K_α is 30.97 keV while L_α has an energy of 4.29 keV. For elements of higher Z, the efficiency for detection of L X-rays will increase rapidly. Further, the cross section for excitation of L X-rays will be much greater than that for K X-rays for these elements. While ultimately a crystal spectrometer would be desirable, it will be some time before it becomes essential.

(3) A NaI(Tl) γ-ray spectrometer, 38 mm diam. $\times$ 30 mm long in the form of an integral assembly is also provided. This permits the detection of nuclear γ-rays. This technique is very powerful for many cases in which the elements sought are below atomic wt. $A = 30$ when the quantitative interpretation of X-ray excitation becomes difficult.

All these facilities generate charged-particle, X-ray or γ-ray spectra in the form of pulse height distributions. If the beam is scanned over an area 100 $\mu \times 100$ μ, i.e. 20×20 beam spot widths, one has potentially 400 such spectra. This represents a formidable data handling problem if quantitative results are to be obtained. It is not beyond the capability of a small computer if a limited selection of spectral lines is made using analogue techniques.

For a more qualitative but valuable presentation the following technique has been used. The waveforms driving the proton beam in its X and Y scan are applied to a cathode ray oscilloscope so that the two beams move in synchronisation. Signals from the detector are used to brighten up the oscilloscope whenever the selected radiation is detected. A storage oscilloscope is useful for temporary view-

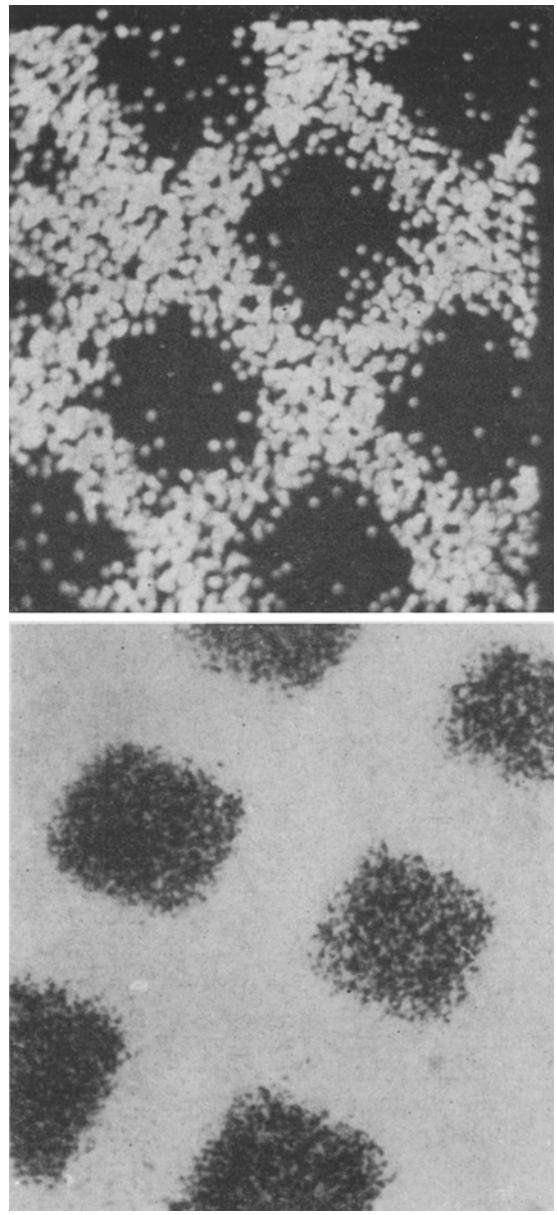

Fig. 4. Photograph of the oscilloscope image obtained by back-scattering of Protons from a copper grid

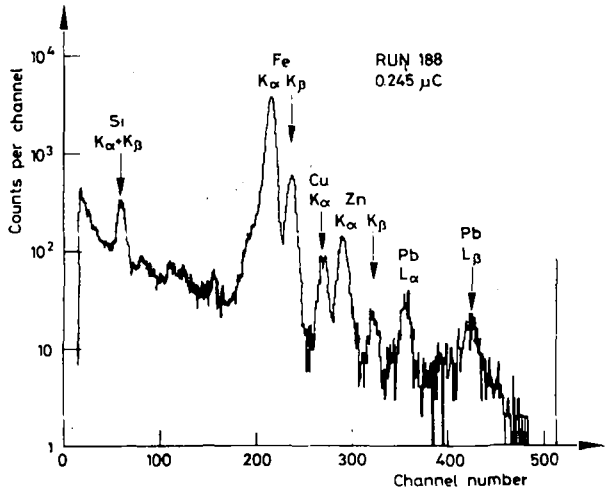

Fig. 5. X-ray spectrum from bombardment of an area 165 μm × 165 μm of a sample of slag

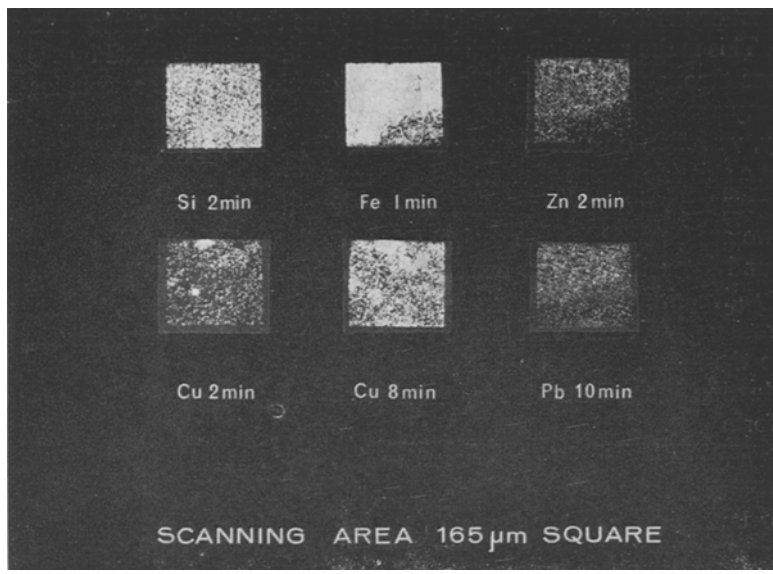

Fig. 6. Photographs of the oscilloscope images obtained by observation of characteristic X-rays as the proton beam is scanned over an area 165 μm square of a sample of slag

ing of the results or a photograph may be taken. This technique produces a map of the distribution of the element in question. As a demonstration of this, a copper grid (bars 24 μm wide, separating holes with 40 μm sides) was used as a test specimen The grid was mounted on a carbon backing. Two sets of measurements

were made, the first using back-scattered protons, the second detecting the Cu K X-rays. The results are shown in Fig. 4. Clearly, the width of the Cu bars is increased by the spot widths on both sides at the expense of the separating holes.

Another specimen examined in this way is of furnace slag. Fig. 5 shows the observed X-ray spectrum. Gates were set around the lines of Si, Fe, Cu, Zn and Pb. The observed maps are shown in Fig. 6. Of particular interest are the tiny specks of copper of diameter 15 μm. These appear in Fig. 6 both in the two- and eight-min exposures.

Once the distributions are mapped, it is possible to choose the deflection voltages to bombard a spot of interest and obtain quantitative data. Clearly also, the average composition over the whole area scanned is given by the total X-ray spectrum.

Background problems in proton excitation of X-rays

In electron-excited X-ray production, direct bremsstrahlung is the major source of background. For proton excitation, the corresponding effect is reduced by a factor (mass of electron/mass of proton).[2] Unfortunately, it appears that a second order effect produces a background which may be the limiting factor in a number of cases. This is the radiation arising from the delta rays produced by the passage of protons through the sample. Since the production of delta rays is inseparable from X-ray production and varies with beam energy and particle type in an identical way, variation on these parameters provides no solution, although it is possible that a suitable choice of viewing angle may help. If the medium under analysis is homogeneous again no manipulation of target thickness is of any value. However, if we are bombarding a specimen deposited on a backing of our choice the background intensity may be considerably influenced. In the backing the delta rays may give rise to characteristic radiation of the elements present and also bremsstrahlung. A choise of a low Z backing can make the former negligible and minimize the latter. This choice is confirmed in that the cross-section for delta-ray production is shown by HUUS, BJERREGAARD and ELBEK[18] to have the following form

$$d\sigma(E_\delta) = \text{const} \cdot E_p^4 Z^4 E_\delta^{-7} dE_\delta$$

while for bremsstrahlung we have

$$d\sigma(E_\gamma) = \text{const} \cdot Z^2 E_\gamma^{-1} E_\delta^{-1} dE_\gamma$$

The strong dependence on the Z of the backing is clearly shown.

One possible backing material is carbon which can be prepared in thin films < 5 μg/cm^2 as is customarily used in Nuclear Physics as a target backing. We have examined a number of such carbons prepared by two different laboratories. A typical X-ray spectrum from such a carbon foil is shown in Fig. 7. Clearly, it

contains Fe, Cu, Zn, Ca, K and other materials in amounts corresponding to some tens of nanograms. Our techniques laboratory has prepared some 'special' carbons and X-ray spectra for these are shown in Fig. 7. Superimposed is the spec-

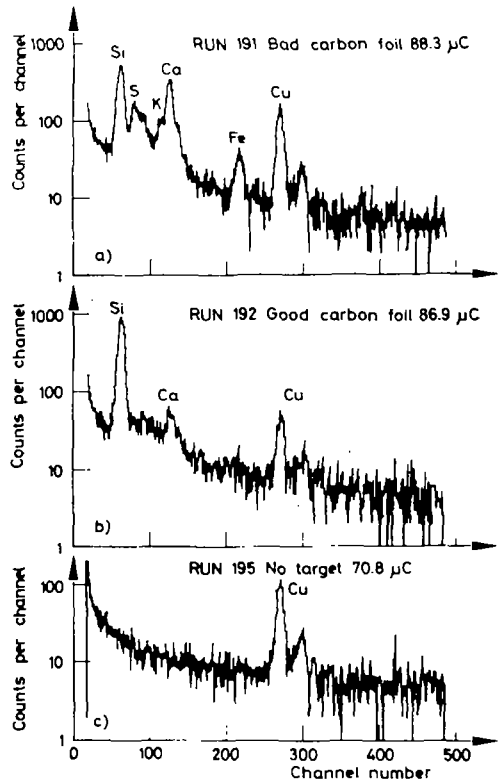

Fig. 7. X-Ray spectra observed during the bombardment of carbon foils. a — Spectrum taken with a 'standard' C foil; b — spectrum taken with a specially prepared high-purity foil; c — spectrum observed with no C foil in position

trum observed for the same proton charge with an empty frame. Clearly, only minute amounts of potassium, calcium and sodium remain, apart from the Cu appearing independently of the carbon. On carbons such as this little difficulty would be experienced in observing iron down to one nanogram/cm^2. With our microbeam, we have easily observed amounts of Fe hit by the beam as small as 10^{-11} g with peak-to-background 5 : 1 and we are fairly confident that this limit could be considerably reduced.

References

1. S. RUBIN, V. K. RASMUSSEN, *Phys. Rev.*, 78 (1950) 83.
2. S. RUBIN, T. O. PASSELL, L. E. BAILEY, *Anal. Chem.*, 29 (1957) 736.
3. S. RUBIN, in Treatise on Analytical Chemistry (KOLTHOFF and ELVING, Eds), Interscience, New York, 1963, p. 2075.
4. J. P. BUTLER, Proc. Symp. on Radiochemical Analysis, Salzburg, 1964, IAEA, Vienna, 1965, p. 391.
5. T. B. PIERCE, P. F. PECK, D. R. A. CUFF, *Analyst*, 92 (1967) 143.
6. P. B. PRICE, J. R. BIRD, *Nucl. Instr. Methods*, 69 (1969) 277.
7. D. M. POOLE, J. L. SHAW, Harwell Report AERE-R 5918, 1968.
8. D. M. POOLE, private communication.
9. A. R. HILL, Mullard Research Labs., Annual Review '67/'68, p. 49.
10. J. H. M. DELTRAP, Correction of spherical aberration of electron lenses, Thesis, Cambridge, 1964.
11. A. D. DYMNIKOV, T. FISHKOVA, S. YAVOR, *Sov. Phys.—Tech. Phys.*, 10 (1965) 340.
12. P. W. HAWKES, Proc. of Workshop on Electron Microscopy, 1966, ANL-7275, p. 32.
13. P. W. HAWKES, Quadrupole Optics Vol. 42 of Springer Tracts in Modern Physics, Springer-Verlag, Berlin, 1966.
14. J. K. COBB, J. J. MURRAY, *Nucl. Instr. Methods*, 46 (1967) 99.
15. J. W. GARDENER, D. WHITESIDE, Rutherford Lab. Repts. NIRL/M/21, 1961 and NIRL/M/44, 1963.
16. P. GRIVET, A. SEPTIER, *Nucl. Instr. Methods*, 6 (1960) 126 and 243.
17. G. D. ARCHARD, *Rev. Sci. Instr.*, 29 (1958) 1049.
18. T. HUUS, J. H. BJERREGAARD, B. ELBEK, *Kgl. Danske Vid. Selsk., mat.-fys. Medd.*, No. 17 (1956) 30.